

# ON THE ROLE OF JACK-UP HULL-IN-WATER RADIATION IMPEDANCE DURING SPUDCAN IMPACTS WITH THE SEABED

K.R. Drake\* and Y. Zhang

Noble Denton Marine Assurance and Advisory  
DNV GL – Oil & Gas

*\*corresponding author: kevin.drake@dnvgl.com*

## ABSTRACT

A simplified structural model has been developed to investigate implications of the Cummins equation for time domain simulations of jack-up rig spudcan impacts with the seabed when going on location. Values of frequency-dependent hydrodynamic added mass and radiation damping are computed for a representative hull using a three-dimensional panel code. Attention is given to estimating high-frequency asymptotes for added mass and the computation of retardation functions. It is demonstrated that the retardation functions play an insignificant role during spudcan impacts. The principal hydrodynamic forces are associated with the high-frequency asymptotes of added mass and hull deceleration. Differences in the distribution of kinetic energy into leg axial and leg bending modes for single leg heave and pitch impacts are investigated. Possible refinements are discussed, such as the use of phase co-factors, to assess concurrent components of rigid body velocities at impact.

**KEY WORDS:** Cummins equation; jack-up; spudcan impact; phase co-factors.

## INTRODUCTION

There is an industrial need to have a good understanding of going on location issues for jack-up rigs with the hull in the water. To analyse the risks involved, time domain simulations are required in order to represent the important nonlinearities in the interaction between the leg spudcans and the seabed. However, the hydrodynamic added mass and damping properties of a jack-up hull are dependent upon the direction and frequency content of the hull motion. In the general case, this frequency dependence cannot be represented in the time domain with constant hydrodynamic coefficients.

There are two main parts in the hydrodynamic loading on the hull: the first is associated with the diffraction problem, namely the loading on the hull in waves in the absence of motions; the second is associated with the radiation problem, namely the loading on the hull brought about by the motion of the hull in otherwise still water.<sup>1</sup> The two parts are combined using the principle of linear superposition. The latter is valid for the low to moderate sea conditions associated with going on location. Time histories of the diffraction loading in irregular seas can be computed in a straightforward manner using standard inverse Fourier transform techniques. Potentially the radiation problem is less straightforward, since it depends on the unknown motion of the hull during the course of spudcan impacts with the seabed.

Tackling the radiation problem in the time domain is the principal hydrodynamics challenge to be addressed if full length time domain simulations of going on location are to be produced. In this paper the key focus is upon the role of radiation impedance during short duration isolated episodes of spudcan impacts with the seabed. The aim is to provide guidance on simplifying approximations that may be applied for the episodic modelling of impacts.

## BACKGROUND

The purpose of defining limiting conditions (or motions) for going on location is to help manage the risk of damage to legs and jacking systems caused by severe impact between a descending spudcan and the seabed. Well established rigorous methods of analysis for spudcan impacts have been in use for more than two decades (e.g. Miller et al. [2], Lai et al. [3], Smith et al. [4]). Typically these methods involve two main stages. In the first stage, a linearised frequency domain analysis of vessel motions is carried out for pre-

---

<sup>1</sup> The fluid force acting on a body that is moving harmonically with unit velocity amplitude and generating surface waves is termed radiation impedance (e.g. Damaren [1]).

impact conditions. This involves taking into account diffraction and radiation effects of the jack-up hull along with estimates of additional damping due to nonlinear fluid drag forces acting on the legs. Short term statistical properties of a stationary random process are then applied to make predictions of expected extreme values of vessel motions and spudcan impact velocities. In the second stage, the extreme response velocities are applied as initial values to a separate ‘barstool’ structural model with linear elastic properties and nonlinear representations of seabed contact and geotechnical behaviour. The separate analyses of the pre-impact and impact stages seem justifiable for the investigation of isolated impact episodes when the impact timescale is short compared with the characteristic period of pre-impact motion responses.

DNV-RP-C104 [5] provides a simplified method that may be suitable for initial assessments. It assumes that during impact all the kinetic energy due to angular motion of the vessel is transferred into strain energy within a single impacting leg. The lower end of the leg is stopped immediately upon impact as the seabed is assumed to be rigid. The vessel is constrained to only roll, or pitch, about its centre of gravity. This artificial kinematic constraint suppresses horizontal and vertical translation of the vessel and enforces leg axial forces and bending moments to peak simultaneously.

Chakrabarti [6] provides comparisons of the DNV simplified method with the results obtained from unconstrained ‘barstool’ finite element models for legs impacting on different types of seabed ranging from rock through to hard clay, soft clay and sand. As expected, a softer seabed leads to reduced impact forces for a given seastate. However, it was also shown that the simplified method could lead to under-prediction of bending moments when the dynamic effects of leg inertia become significant. These findings are also evident in the earlier work of Miller et al. [2], Lai et al. [3] and Smith et al. [4].

The admissibility of hull translation in a ‘barstool’ structural model leads typically to a significant time lag between leg axial forces (earlier) and leg bending moments (later). This is a feature of spudcan impact models with both linear and nonlinear representations of the seabed impact. We believe that this can be most easily understood from consideration of the modal response of a linear elastic structure when subjected to finite initial velocities and zero initial displacements (i.e. boundary conditions at the onset of impact). Consideration of the general case is given in Appendix A whilst a specific example is considered in the main text. It can be shown that the time delay is associated with the difference in natural frequencies between vibration modes dominated by leg bending (lower) and those dominated by leg axial deformations (higher) when the spudcan is latched (artificially) onto the seabed.

Kreuzer et al. [7] present the development of a time-domain model for the computation of leg impact forces caused by jack-up motions in irregular waves. A total of 3000 realizations, each of 15 minutes duration, were carried out with legs being lowered at a constant speed of 0.5 m/min. The case considered was a third generation jack-up vessel for wind farm installation with attention given specifically to the case of coupled sway-heave-roll motion in beam seas. According to our knowledge this appears to be the first published paper to describe a continuous time domain representation of leg touchdown in irregular waves due to vessel motions.

The possible benefits of a continuous time domain representation include the capability to represent non-stationary aspects of the system prior to impact, perhaps due to changes in centre of gravity and radii of gyration due to leg lowering. Other benefits include the representation of time-varying wave loads during the course of impacts and statistical variation in the components of rigid body velocity at the time of impact. However, in cases where the pre-impact vessel motions can be considered as a stationary random process and the timescale of impacts is very short compared to wave periods, the benefits of analyses in the frequency and probability domains may well outweigh the possible benefits of analyses in the time domain. Aside from issues of computational effort, Hutchison [8] argues the fundamental point that the frequency and probability domain methods have the status of population statistics in contrast with the sample statistics of time domain simulations.

## THEORETICAL FORMULATION OF HULL-IN-WATER RADIATION IMPEDANCE

Cummins [9] derived a linear time domain equation to represent the dynamics of a large floating marine structure in waves. An inviscid, incompressible fluid undergoing irrotational flow is assumed. The equation

is referred to as the Cummins equation. Following the exposition and nomenclature of Chen et al. [10], it has the following form for a floating rigid body:

$$[\mathbf{M} + \mathbf{A}(\infty)]\ddot{\mathbf{x}}(t) + \int_0^t \mathbf{h}(t-\tau)\dot{\mathbf{x}}(\tau)d\tau + \mathbf{K}\mathbf{x}(t) = \mathbf{f}^{exc}(t) \quad (1)$$

where,  $\mathbf{x}$  is the vector of the rigid body degrees of freedom and a dot denotes time derivative;  $\mathbf{M}$  is the mass matrix;  $\mathbf{A}(\infty)$  is the constant positive-definite infinite-frequency added mass matrix; the kernel of the convolution term  $\mathbf{h}(t)$  is the matrix of retardation functions and is linked to fluid memory effects;  $\mathbf{K}$  is the hydrostatic stiffness; and  $\mathbf{f}^{exc}(t)$  is the vector of wave excitation forces and moments that vary with time,  $t$ .

The retardation functions can be obtained by evaluating the following integral:

$$\mathbf{h}(t) = \frac{2}{\pi} \int_0^\infty \mathbf{B}(\omega) \cos(\omega t) d\omega \quad (2)$$

where  $\mathbf{B}(\omega)$  is the positive definite matrix of hydrodynamic radiation damping coefficients at frequency  $\omega$ .

Hydrodynamic coefficients can be readily obtained over a finite range of frequencies using three-dimensional panel codes. These are based on the use of boundary integral methods to solve the potential flow problem. Greenhow [11] provides guidance on how the computed hydrodynamic coefficients may be used to provide estimates of high-frequency asymptotes for added mass and high-frequency approximations for radiation damping.

#### HIGH-FREQUENCY ASYMPTOTES FOR ADDED MASS OF REPRESENTATIVE HULL

Figure 1 shows the panel mesh for a hydrodynamic model of a representative hull. The main simplification compared to a more realistic model of a jack-up rig is the omission of leg wells. Hydrodynamic coefficients have been computed at 30 different frequencies over the range 0.105 to 1.795 rad/s (0.0167 to 0.2857 Hz) using AQWA [12]. Figure 2 shows the pitch added mass (inertia) over the range of frequencies considered.

Greenhow [11] has shown that if added mass coefficients are known over the frequency range  $0 \leq \omega \leq \sigma$  then an estimate of the high-frequency asymptote for the added mass coefficient  $A_{ij}$  may be obtained from the following approximation:

$$A_{ij}(\infty) \approx \frac{1}{2} A_{ij}(\sigma) + \frac{1}{4\sqrt{\sigma}} \int_0^\sigma \frac{A_{ij}(\omega)}{\sqrt{\omega}} d\omega \quad (3)$$

Table 1 shows the results obtained from numerical integration of the computed added mass coefficients with different upper limits for the integral in (3). The results show that the estimates of the high-frequency asymptotes for heave and pitch are rather insensitive to the upper limit for the values considered. The added mass results for surge are slightly more sensitive to the upper limit, however, it is noted that the magnitudes are much smaller than those for heave, so the issue of reduced accuracy is less important.

#### RETARDATION FUNCTIONS FOR REPRESENTATIVE HULL

Spline interpolation was used to provide values of radiation damping at 71 frequencies with uniform spacing from zero up to 1.795 rad/s. The retardation functions were computed at time intervals of 0.01s using the trapezoidal rule. Figure 3 shows the pitch radiation damping over the range of frequencies considered and Figure 4 shows the corresponding retardation function that has been computed using (2).

The convolutions in (1) can become very time consuming for long simulations. Substantial improvements in computational efficiency can be obtained by approximating the convolutions with a state-space model (e.g.

[7], [10]). However, such an approach is not necessary for the short duration simulations considered in this paper.

### SIMPLIFIED STRUCTURAL MODEL

Figure 5 provides an illustration of a simplified two-dimensional linear elastic structural model that we consider to be sufficient for the purposes of investigating the effects of hull hydrodynamics. A rigid hull is connected to a single leg which has cross-sectional area  $A$  and second moment of area  $I$ . The leg material has a modulus of elasticity  $E$ . The horizontal offset of the leg from the hull centre of gravity is  $s$  and the length of the leg is  $L$ . The model has five degrees-of-freedom (5DOF): surge, heave and pitch of the hull ( $u_1, v_1, \theta_1$ ) and horizontal and vertical translation of the bottom of the leg ( $u_2, v_2$ ). The hull has hydrostatic restoring stiffness  $k_{v1}$  in heave and  $k_{\theta1}$  in pitch. Vertical and horizontal springs with stiffness  $k_{v2}$  and  $k_{h2}$  are provided at the bottom of the leg. It may be shown that the 5DOF model has the following stiffness matrix:

$$\mathbf{K} = \begin{bmatrix} \frac{3EI}{L^3} & 0 & \frac{3EI}{L^2} & -\frac{3EI}{L^3} & 0 \\ 0 & \left(\frac{EA}{L} + k_{v1}\right) & \frac{EAs}{L} & 0 & -\frac{EA}{L} \\ \frac{3EI}{L^2} & \frac{EAs}{L} & \left(\frac{3EI}{L} + \frac{EAs^2}{L} + k_{\theta1}\right) & -\frac{3EI}{L^2} & -\frac{EAs}{L} \\ -\frac{3EI}{L^3} & 0 & -\frac{3EI}{L^2} & \left(\frac{3EI}{L^3} + k_{h2}\right) & 0 \\ 0 & -\frac{EA}{L} & -\frac{EAs}{L} & 0 & \left(\frac{EA}{L} + k_{v2}\right) \end{bmatrix} \quad (4)$$

A computer program has been written in Fortran 90 in order to apply the Cummins equation to the analysis of the representative rig model with prescribed initial conditions and without incident waves ( $\mathbf{f}^{exc} = 0$ ). The constant acceleration method, as described by Clough and Penzien [13], has been implemented and extended to include the convolutions associated with the retardation functions. The program has been validated against the retardation function and transient oscillations presented by Damaren [1] and Chen et al. [10] for the case of a heaving hemisphere.

### INFLUENCE OF HULL RADIATION IMPEDANCE ON RESPONSES BEFORE AND AFTER IMPACT

Figures 6 and 7 show the transient oscillations associated with initial displacements and initial velocities in heave and pitch with the vessel in the free floating condition. The model parameters are given in Table 2. Only on-diagonal high-frequency asymptotes for added mass coefficients and on-diagonal retardation functions for heave and pitch were incorporated in the model; hydrodynamic effects in surge and coupling between the degrees of freedom were considered to be negligible. The time increment in the simulations was 0.01s. It can be seen that in the free floating condition the heave response is much more heavily damped than the pitch response, as expected.

Figures 8 and 9 show the transient oscillations due to initial velocities associated with rigid body heave and pitch motion at the onset of impact. The leg is connected to horizontal and vertical springs representing the contact with the seabed. This is the only change that was applied to the model parameters when comparing with the cases considered in Figures 6 and 7. The values for spring stiffness have been set equal to one quarter of the axial stiffness of the leg in order to generate typical impact durations of around 1s. Results are presented with and without the effects of retardation functions being included. The two sets of results in each figure are shown to be indistinguishable for the short duration whilst the vertical spring at the seabed is in compression. Differences arise only at later stages beyond the range of practical interest.

The fact that the retardation functions have no significant effect for the short period after impact is directly attributable to the minimal amounts of radiation damping at frequencies associated with hull responses when

the leg is in contact with the seabed. For the case that has been considered, it is evident that the retardation functions are only of importance for time domain simulations in the free floating condition prior to impact.

#### FREE VIBRATION ANALYSIS WITH HIGH-FREQUENCY ASYMPTOTES FOR ADDED MASS

With the retardation functions having a negligible role after impact, the constant coefficient mass and stiffness matrices that are in place for a short duration after impact present a standard eigenvalue problem, albeit momentarily. The principal hydrodynamic forces during this time are associated with the high-frequency asymptotes for the added mass coefficients and the decelerations of the rig. Perhaps this aspect has not always been understood by practitioners, since in [2] it is stated that the added mass coefficients were based on a wave period of 10s.

Figure 10 shows the first three modes of vibration for the representative hull with its leg in contact with the seabed, as considered in the analysis results presented in Figures 8 and 9. We have termed these modes as inverted pendulum, leg bending and leg axial. The natural frequencies of 1.44 rad/s ( $T_2 = 4.37\text{s}$ ) for the leg bending mode and 3.67 rad/s ( $T_3 = 1.71\text{s}$ ) for the leg axial mode can be considered in conjunction with Figure 3 in order to confirm that radiation damping is minimal for these modes.

Table 3 shows the proportions of kinetic energy that are directed into these modes in the separate cases of heave and pitch impacts. It is shown that most of the kinetic energy in the pitch impact is directed to the leg axial mode whilst most of the energy in the heave impact is directed to the leg bending mode. Details of the analysis methodology are given in Appendix A.

The tendency for a single leg heave impact to cause leg bending can be understood by considering an abstract case; a jack-up rig with a rigid leg latches onto a fixed pivot at impact in the absence of hydrostatic restoring effects. In this case there is conservation of angular momentum about the pivot. Horizontal velocity at the centre of gravity arises when the rig rotates about the pivot. The associated horizontal momentum is caused by a horizontal impulse being generated at the pivot. The effect would be moderated by compliance of the leg and seabed.

#### MOST PROBABLE COMPONENTS OF RIGID BODY MOTION AT IMPACT

Frequency-domain analyses are often used to generate estimates of independent extreme values of rigid body motions and spudcan velocities. These may then be applied in a conservative manner as concurrent initial velocities to a ‘barstool’ structural model for the investigation of spudcan impacts with the seabed. A more realistic approach might be to consider the most probable components of rigid body motion associated with the instant of extreme vertical velocity of the impacting spudcan. The phase co-factors methodology developed by Hutchison [8] is well established for other applications and would seem to be highly suitable for use in spudcan impact studies. An alternative approach is outlined in Appendix B. The authors propose further investigation regarding the applicability of both methods to spudcan impact analyses.

#### CONCLUSIONS

It has been demonstrated for a representative hull that the retardation functions in the Cummins equation play an insignificant role during spudcan impacts with the seabed. The principal hydrodynamic forces acting on the hull are associated with the high-frequency asymptotes of added mass coefficients and the hull deceleration.

For the cases considered, it has been shown that single leg pitch impacts direct most of the kinetic energy into leg axial modes, whilst single leg heave impacts direct most of the kinetic energy into the leg bending modes. The authors recommend further assessment to define most probable concurrent components of rigid body motion associated with extreme spudcan velocities.

## REFERENCES

- [1] Damaren, C.J. Time-domain floating body dynamics by rational approximation of the radiation impedance and diffraction mapping. *Ocean Engineering*, 2000, 27, 687-705.
- [2] Miller, B.L., Frieze, P.A., Lai, P.S.K., Lewis, T.C. and Smith, I.A.A. Motion and impact responses of jackups moving onto location. 25<sup>th</sup> Annual Offshore Technology Conference, Houston, 1993, OTC 7301, 389-398.
- [3] Lai, P.S.K., Lewis, T.C., Frieze, P.A., Miller, B.L. and Smith, I.A.A. Limiting motions for jack-ups moving onto location. Jack-up Platform Conference 1993. City University, London.
- [4] Smith, I.A.A., Frieze, P.A., Lai, P.S.K., Lewis, T.C. and Miller, B.L. Evaluation of leg damage risk for jackups going on location. 26<sup>th</sup> Annual Offshore Technology Conference, Houston, 1994, OTC 7530, 195-202.
- [5] DNV Recommended Practice DNV-RP-C104. Self-elevating Units. November 2012.
- [6] Chakrabarti, P. Going on location study for a jack-up rig. Proceedings of the ASME 31<sup>st</sup> International Conference on Ocean, Offshore and Arctic Engineering, 2012, OMAE2012-83034, 1-14.
- [7] Kreuzer, E., Solowjow, E., Qiu, G, Hamman, T., Gabe, J. Leg-seabed interactions of jack-up vessels due to motions in irregular waves. Proceedings of the ASME 33<sup>rd</sup> International Conference on Ocean, Offshore and Arctic Engineering, 2014, OMAE2014-24303, 1-10.
- [8] Hutchison, B.L. Joint seakeeping response processes for determining structural loads. Transactions of the Society of Naval Architects and Marine Engineers, 2002.
- [9] Cummins, W.E. The impulse response function and ship motions. Hydromechanics Laboratory Research and Development Report. David Taylor Model Basin, 1962, Report 1661.
- [10] Chen, M., Eatock Taylor, R., Choo, Y.S. Time domain modelling of a dynamic impact oscillator under wave excitations. *Ocean Engineering*, 2014, 76, 40-51.
- [11] Greenhow, M. High- and low-frequency asymptotic consequences of the Kramers-Kronig relations. *Journal of Engineering Mathematics*, 1986, 20, 293-306.
- [12] AQWA User's Manual, ANSYS, Inc., Release 14.5, October 2012.
- [13] Clough, R.W. and Penzien, J. Dynamics of Structures. Second Edition. McGraw-Hill, 1993.
- [14] Drake, K.R. Wave profile characterisation of green water loading events from model test data. *Applied Ocean Research*, 2001, 23, 187-193.

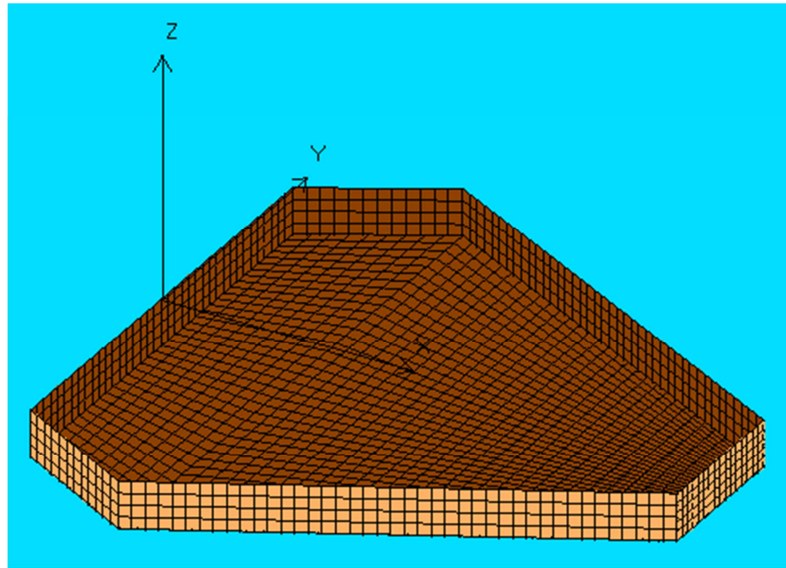


Figure 1 Hydrodynamics panel model (AQWA plot)

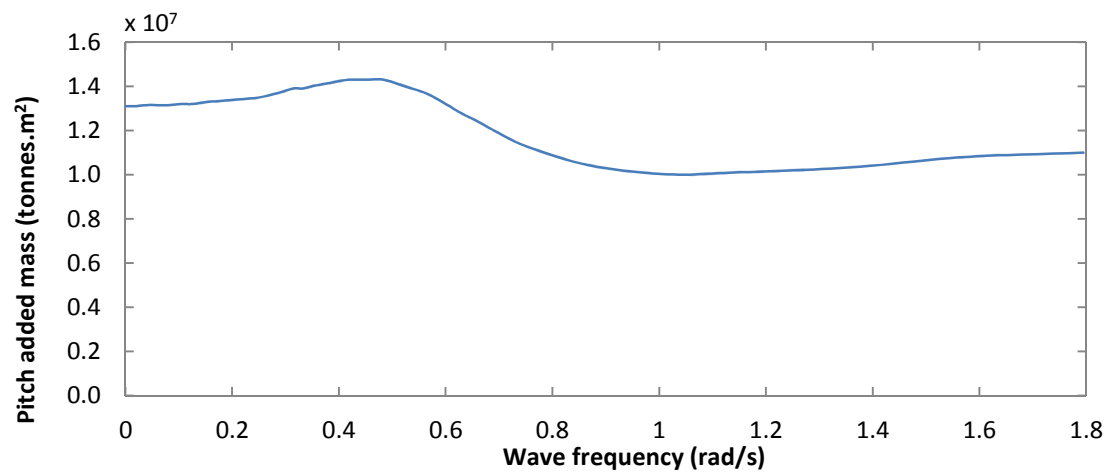


Figure 2 Pitch added mass

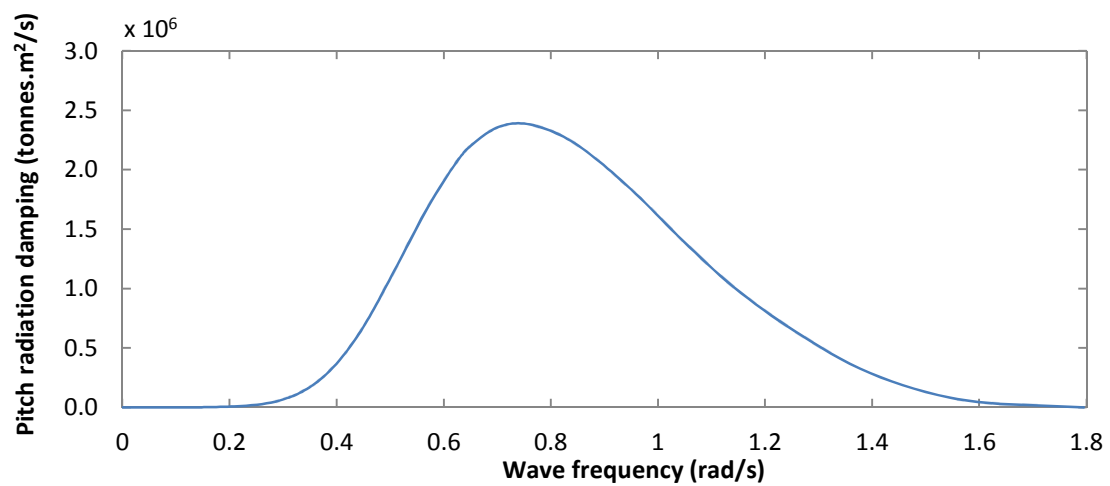


Figure 3 Pitch radiation damping

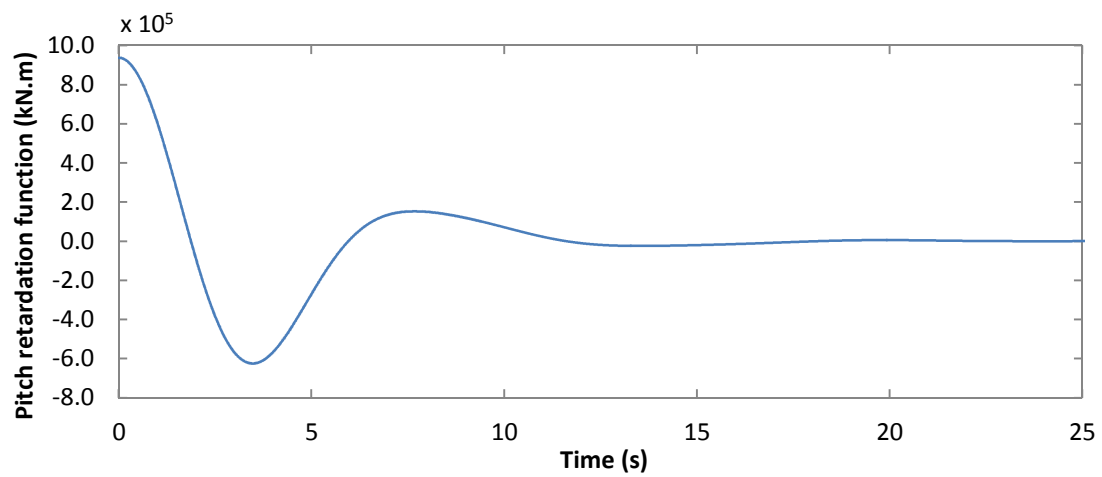


Figure 4 Pitch retardation function

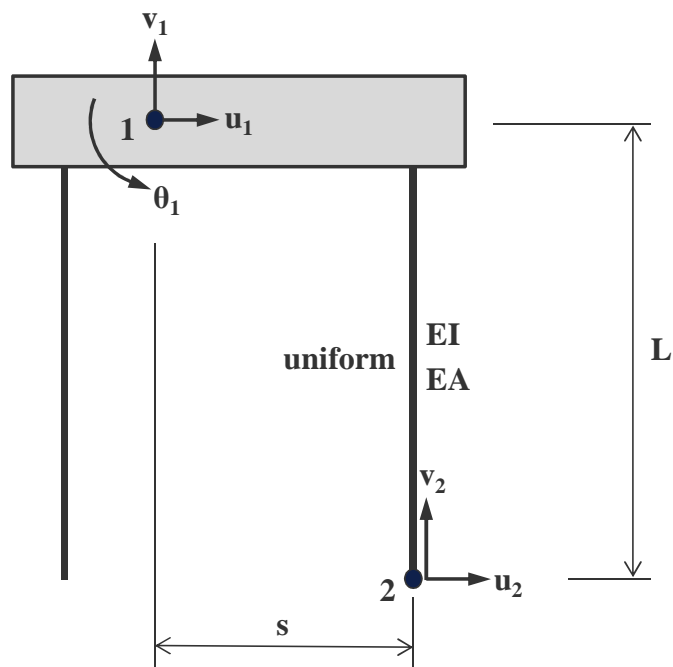


Figure 5 Schematic of simplified 2-D linear elastic structural model

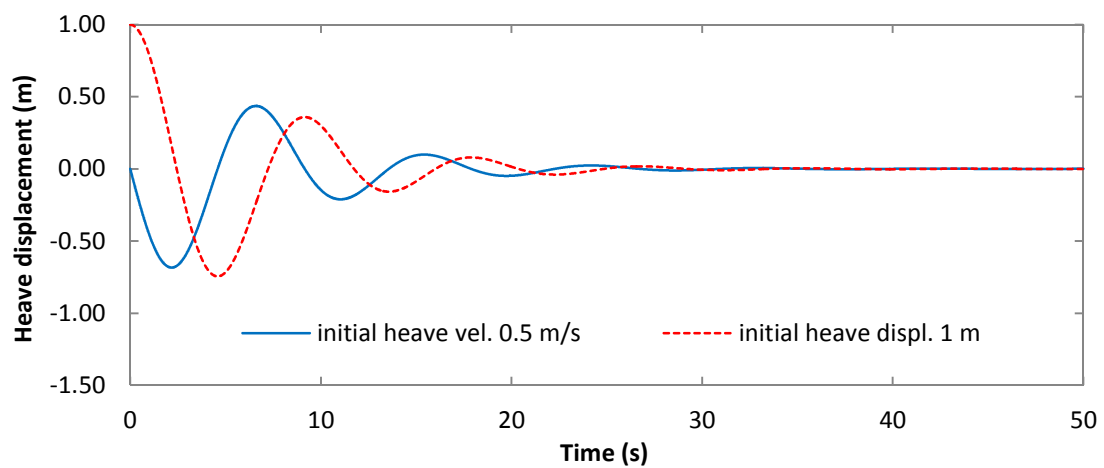


Figure 6 Heave transient oscillations with the vessel in free floating condition



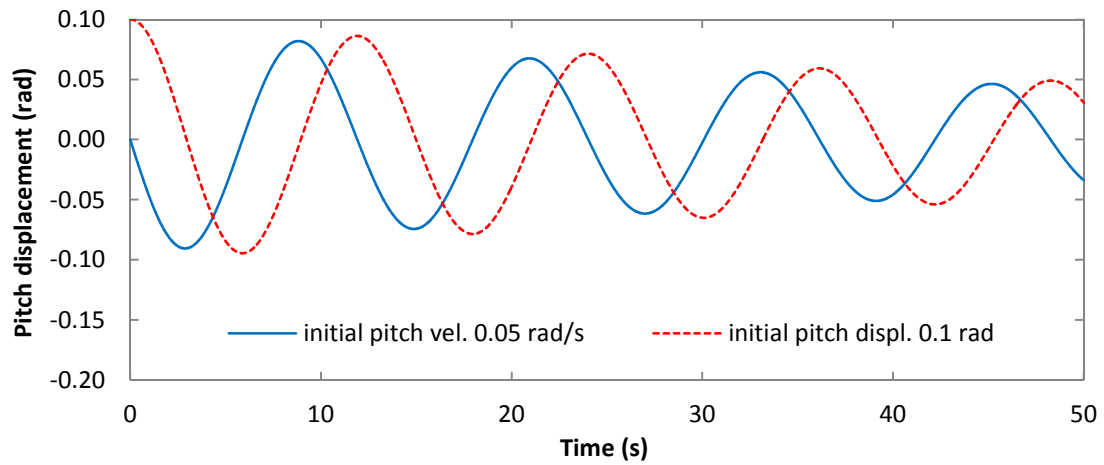


Figure 7 Pitch transient oscillations with the vessel in free floating condition

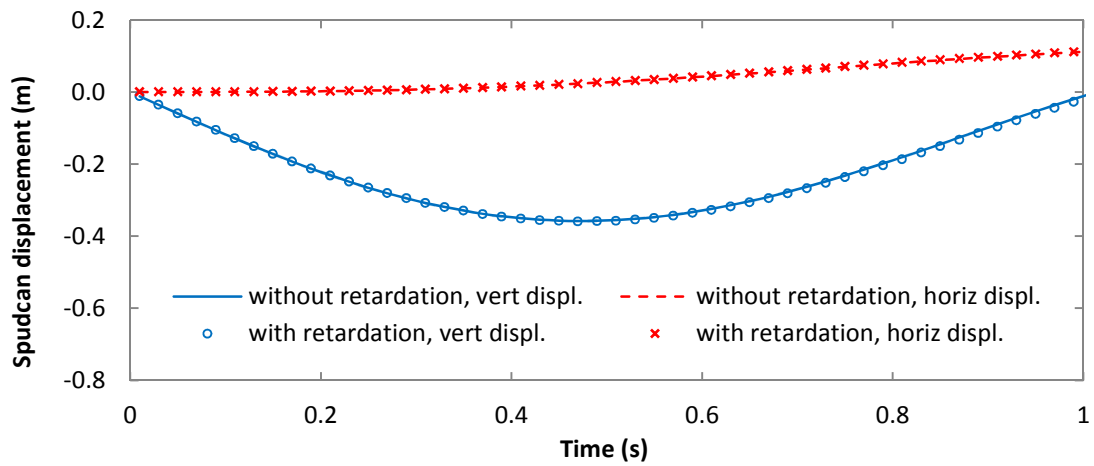


Figure 8 Transient oscillations due to initial heave velocity 1.5 m/s

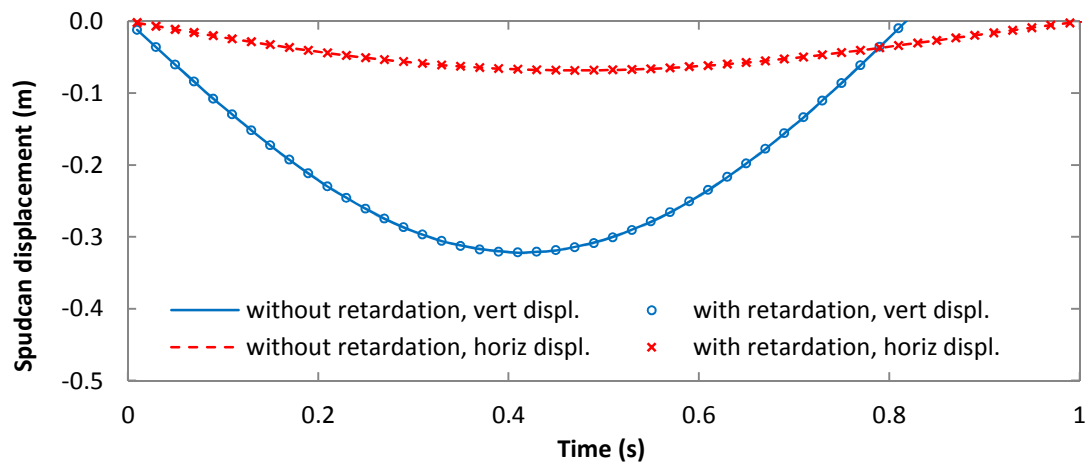


Figure 9 Transient oscillations due to initial pitch velocity 0.05 rad/s

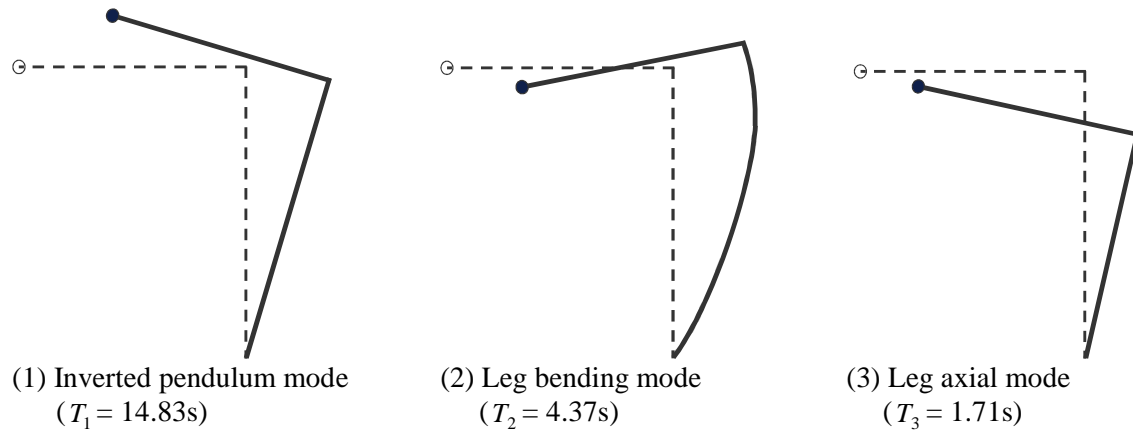


Figure 10 Mode shapes when leg is latched onto seabed

Table 1 High frequency asymptotes for hydrodynamic added mass in surge, heave and pitch			
Frequency $\sigma$ (rad/s)	Surge $A_{11}(\infty)$ (tonnes)	Heave $A_{22}(\infty)$ (tonnes)	Pitch $A_{33}(\infty)$ (tonnes.m <sup>2</sup> )
1.047	$3.31 \times 10^3$	$6.04 \times 10^4$	$1.07 \times 10^7$
1.142	$2.96 \times 10^3$	$6.06 \times 10^4$	$1.08 \times 10^7$
1.257	$2.64 \times 10^3$	$6.11 \times 10^4$	$1.08 \times 10^7$
1.396	$2.37 \times 10^3$	$6.09 \times 10^4$	$1.08 \times 10^7$
1.571	$2.15 \times 10^3$	$6.19 \times 10^4$	$1.10 \times 10^7$
1.795	$2.01 \times 10^3$	$6.25 \times 10^4$	$1.11 \times 10^7$

Table 2 Model parameters	
Hull length (m)	70.36
Hull width (m)	76.00
Hull depth (m)	9.40
Hull draught (m)	6.00
Hull waterplane area (m <sup>2</sup> )	3,620
Hull second moment of waterplane area (m <sup>4</sup> )	$1.22 \times 10^6$
Hull and leg dry mass (tonnes)	22,265
Longitudinal leg spacing (m)	45.72
Transverse leg spacing (m)	47.55
Leg cross-sectional area (m <sup>2</sup> )	0.537
Leg second moment of area (m <sup>4</sup> )	15.373
Leg length, L (m)	70.00
Leg offset, s (m)	30.48
Radius of gyration for hull and legs (m)	37.69

Table 3 Kinetic energy distribution			
Impact case	Inverted pendulum mode	Leg bending mode	Leg axial mode
Heave impact	26.3%	50.4%	23.3%
Pitch impact	16.2%	8.9%	74.9%

## APPENDIX A - RESPONSE OF LINEAR ELASTIC STRUCTURES TO INITIAL VELOCITIES

Applying the modal superposition methods described by Clough and Penzien [13], the time varying vector of structural displacements  $\mathbf{v}(t)$  may be expressed as

$$\mathbf{v}(t) = \mathbf{\Phi} \mathbf{Y}(t) \quad (\text{A1})$$

where  $\mathbf{\Phi}$  is a matrix of mode shape vectors and  $\mathbf{Y}(t)$  is a time-varying vector of principal coordinates. Pre-multiplying by the mass matrix  $\mathbf{m}$  so that we can use the orthogonal properties of mode shapes gives

$$\mathbf{m} \mathbf{v}(t) = \mathbf{m} \mathbf{\Phi} \mathbf{Y}(t) \quad (\text{A2})$$

Now pre-multiply by the transpose of the mode shape vector

$$\mathbf{\Phi}^T \mathbf{m} \mathbf{v}(t) = \mathbf{\Phi}^T \mathbf{m} \mathbf{\Phi} \mathbf{Y}(t) \quad (\text{A3})$$

Solve (A3) to obtain the principal coordinates

$$\mathbf{Y}(t) = \mathbf{M}^{-1} \mathbf{\Phi}^T \mathbf{m} \mathbf{v}(t) \quad (\text{A4})$$

where  $\mathbf{M} = \mathbf{\Phi}^T \mathbf{m} \mathbf{\Phi}$  is the generalised mass matrix, which is diagonal.

The initial velocities for the principal coordinates are given by

$$\dot{\mathbf{Y}}(0) = \mathbf{M}^{-1} \mathbf{\Phi}^T \mathbf{m} \dot{\mathbf{v}}(0) \quad (\text{A5})$$

where the dot denotes differentiation with respect to time.

Ignoring damping effects, the time history of principal coordinate response in the  $i^{\text{th}}$  mode is given by

$$Y_i(t) = \frac{\dot{Y}_i(0)}{\omega_i} \sin \omega_i t \quad (\text{A6})$$

where  $\omega_i$  is the natural frequency of the  $i^{\text{th}}$  mode. Thus, the peak strain energy first occurs in the  $i^{\text{th}}$  mode when

$$t = \frac{\pi}{2\omega_i} \quad (\text{A7})$$

The kinetic energy of the structure is given by

$$\begin{aligned} \frac{1}{2} \dot{\mathbf{v}}^T(t) \mathbf{m} \dot{\mathbf{v}}(t) &= \frac{1}{2} \dot{\mathbf{Y}}^T(t) \mathbf{\Phi}^T \mathbf{m} \mathbf{\Phi} \dot{\mathbf{Y}}(t) \\ &= \frac{1}{2} \dot{\mathbf{Y}}^T(t) \mathbf{M} \dot{\mathbf{Y}}(t) \end{aligned} \quad (\text{A8})$$

Because the generalised mass matrix is diagonal we have

$$\frac{1}{2} \dot{\mathbf{Y}}^T(t) \mathbf{M} \dot{\mathbf{Y}}(t) = \sum_{i=1}^N \frac{1}{2} M_{ii} \dot{Y}_i(t)^2 \quad (\text{A9})$$

where  $\frac{1}{2} M_{ii} \dot{Y}_i(t)^2$  is the kinetic energy in the  $i^{\text{th}}$  mode.

We note that there is no exchange of energy between the modes. There is only exchange between kinetic and potential (or strain) energy within each mode. In general, the modes of vibration will have different natural frequencies and the time taken to reach peak strain energy in each mode will depend upon its natural frequency. Thus, peak strain energies in the various modes will not occur simultaneously.

## APPENDIX B – TRANSIENT WAVE PACKETS ASSOCIATED WITH SPUDCAN IMPACTS

Following the approach given in [14], it may be shown for long-crested random seas that the most probable wave surface profile associated with an event causing extreme vertical velocity of the spudcan is given by the following summation

$$\eta_{\dot{\zeta}}^*(\tau, x) = \frac{\alpha}{\sigma_{\dot{\zeta}}^2} \operatorname{Re} \left\{ \sum_{n=1}^N S_{\eta}(\omega_n) \overline{H_{\dot{\zeta}}}(\omega_n) \exp[i(\omega_n \tau + k_n x)] \Delta \omega_n \right\} \quad (\text{B1})$$

where,  $\eta^*$  is the most probable free surface elevation and the subscript denotes association with spudcan vertical velocity  $\dot{\zeta}$ ; time relative to the extreme event is  $\tau$  and the horizontal position along the wave profile is  $x$ ; the extreme vertical velocity of the spudcan is  $\alpha$  and its variance is  $\sigma_{\dot{\zeta}}^2$ ; the transient wave packet has  $N$  frequency components; the frequency and wave number of the  $n^{\text{th}}$  component are  $\omega_n$  and  $k_n$  respectively and the frequency spacing is  $\Delta \omega_n$ ;  $S_{\eta}(\omega_n)$  is the spectral density of wave surface elevation and  $\overline{H_{\dot{\zeta}}}(\omega_n)$  is the complex conjugate of the linear transfer function between wave elevation (input) and spudcan vertical velocity (output);  $i$  is  $\sqrt{-1}$ .

The associated time history of the rigid body velocity component  $\dot{\xi}$  (e.g. surge, heave or pitch) is given by

$$\dot{\xi}_{\dot{\zeta}}^*(\tau) = \frac{\alpha}{\sigma_{\dot{\zeta}}^2} \operatorname{Re} \left\{ \sum_{n=1}^N S_{\eta}(\omega_n) \overline{H_{\dot{\zeta}}}(\omega_n) H_{\dot{\xi}}(\omega_n) \exp[i\omega_n \tau] \Delta \omega_n \right\} \quad (\text{B2})$$

where  $H_{\dot{\xi}}(\omega_n)$  is the complex linear transfer function between wave elevation (input) and rigid body velocity (output).

Thus, the rigid body velocity component at the time of the extreme event is given by

$$\dot{\xi}_{\dot{\zeta}}^* \Big|_{\tau=0} = \frac{\alpha}{\sigma_{\dot{\zeta}}^2} \operatorname{Re} \left\{ \sum_{n=1}^N S_{\eta}(\omega_n) \overline{H_{\dot{\zeta}}}(\omega_n) H_{\dot{\xi}}(\omega_n) \Delta \omega_n \right\} \quad (\text{B3})$$